Catalysis Letters 48 (1997) 165–171

Investigation of rhodium complexes in micro- and mesoporous materials by computer modeling, FTIR, and ^{31}P MAS NMR

A. Janssen, J.P.M. Niederer and W.F. Hölderich

Department of Chemical Technology and Heterogeneous Catalysis, RWTH Aachen, Worringer Weg 1, D-52074 Aachen, Germany

Received 9 May 1997; accepted 1 September 1997

Tetracarbonyldichlororhodium(I) $[Rh(CO)_2(\mu\text{-}Cl)]_2$ entrapped in faujasite type zeolites reacted with phosphines $PMe_{3-x}Ph_x$ at 393–463 K to a different extent. Although according to computational studies phosphines with $x < 2$ should be small enough to enter the micropore system, the reaction was in no case complete and led to a mixture of products as observed by IR spectroscopy. Furthermore surface-bonded rhodium carbonyl complexes were synthesized in mesoporous aluminium-containing MCM-41 material by reacting acetylacetonatodicarbonylrhodium(I) $[Rh(acac)(CO)_2]$ with Brønsted-acidic centers under formation of a chemically bonded $[Rh(CO)_2]$-species and acetylacetone according to IR spectroscopy. The corresponding surface-bonded phosphine complex $[(O_s)_x\text{–}Rh(chiraphos)]$ was synthesized and identified with IR and ^{31}P MAS NMR spectroscopy.

Keywords: zeolites, MCM-41, HUSY, rhodium complexes, heterogenization, IR spectroscopy, NMR spectroscopy, computer modeling

1. Introduction

The immobilization of homogeneous catalysts on amorphous carriers, which is supposed to combine the advantages of homogeneous catalysts with the easy separability of heterogeneous ones, has been a field of research for some time [1–3]. It includes among others the approach of so-called surface organometallic chemistry, i.e. a direct chemical bond between surface atoms of the support and the central metal of an organometallic complex is present [4]. This approach was, for example, employed in zeolite chemistry by Schwartz et al. in the reaction of trisallylrhodium $[Rh(allyl)_3]$ with Brønsted-acidic sites in a HNaY zeolite [5]. Recently, Thomas et al. synthesized surface-bonded titanium half-sandwich complexes in mesoporous all-silica MCM-41 material [6].

A second approach of interest in zeolite chemistry is the ship-in-a-bottle immobilization of metal complexes, i.e. the complex is prepared inside a suitable microporous framework and immobilized by sterical hindrance as it is too large to leave the framework [7,8]. This principle has been used to prepare several intrazeolite complexes, for example phthalocyanine [9], salen [10,11], carbonyl [12,13], and phosphine [14,15] complexes. Depending on the conditions, complexes occluded in zeolites often react as well with ligands as with the inner surface of the support [16].

In our study, we investigated the possibility to use dealuminated microporous zeolite Y as a host for rhodium ship-in-a-bottle complexes containing bulky phosphines like chiraphos (2,3-bis-(diphenylphosphino)-butane). For this purpose, we have employed computer modeling and in situ FTIR methods. In a second approach, we wanted to prepare surface-bonded rhodium phosphine complexes in mesoporous materials like Al-containing MCM-41, for example. Again, in situ FTIR besides ^{31}P MAS NMR techniques have been used for characterization.

2. Materials and methods

Carrier materials used were a commercial NaY (Si/Al = 2.7, Degussa), microporous $SiCl_4$-dealuminated zeolite Y (Si/Al > 150, designated DDAY), micro- and mesoporous commercial steam-dealuminated zeolite Y (Si/Al = 30, PQ, designated HUSY), all-silica MCM-41 (pore radius = 18 Å, prepared according to refs. [17–19], designated Si-MCM-41), Al-containing MCM-41 (Si/Al = 30, pore radius = 18 Å, prepared according to refs. [17–19], designated Al-MCM-41), and sodium ion-exchanged Al-containing MCM-41 (designated Na-MCM-41).

The dealuminated zeolites were washed with a HCl solution in order to remove so-called extra framework alumina species formed during the dealumination process which could block the micropores of the zeolites. All materials were characterised by N_2 adsorption, XRD, FTIR and ICP AES measurements.

In the ship-in-a-bottle experiments, zeolite wafers were loaded with $[Rh(CO)_2(\mu\text{-}Cl)]_2$ via sublimation in vacuum at room temperature with approximately one molecule per four supercages (i.e. 0.63 mg per 10 mg zeolite). An excess of phosphines was added repeatedly via gas phase. In the experiments in order to prepare surface-bonded rhodium complexes, $[Rh(acac)(CO)_2]$ and phosphines were added via sublimation or as a methylenechloride solution to the carrier.

Computational studies were carried out by the CATALYSIS 4.0 software of Biosym/msi on an IRIS Indigo workstation. Due to the forcefield used, the zeolite fragments were considered as all-silica structures without cations. Therefore, only the van-der-Waals forces contribute to the energy of a given host/guest assembly. The optimized assembly energies along a forced diffusion path were documented as energy-versus-framework diagrammes.

IR studies were carried out with the help of specially designed transmission cells [20] in a Nicolet 510 spectrometer. The cells allowed the heating and handling of self-supported wafers of pressed zeolite material (approximately 10 mg/cm^2) under Schlenk technique conditions. The wafers were dehydrated in vacuo until they were dry (IR control) at 673 K before loading.

^{31}P MAS NMR spectra were recorded ex situ with a Bruker AC 300 spectrometer (^{31}P: 121 MHz, $\pi/2$-impulse: 4.8 μs, repetition time: 20 s, MAS frequency: 4.4 kHz).

3. Results and discussion

3.1. Ship-in-a-bottle approach: computer modeling

The energy change of a zeolite/phosphine assembly was calculated while the guest molecule was forced stepwise through a rigid faujasite fragment consisting of two supercages saturated with hydroxyl groups (figure 1). The assembly energy was optimized in each single position.

Figure 2 contains four resulting energy diagrammes. The guest molecules are the phosphine ligands methylphenylpropylphoshine (PMePhPr), dimethylphenylphosphine (PMe_2Ph), methyldiphenylphosphine ($PMePh_2$), and triphenylphosphine (PPh_3), respectively.

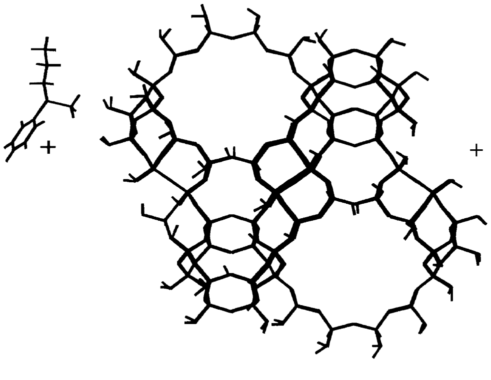

Figure 1. Guest molecule and faujasite fragment host with start (left) and end point (right) of forced diffusion path.

In all cases, there is an energy decrease of the host/guest assembly in the beginning because of attractive van-der-Waals interactions as there is no contact between host and guest at the starting point. PMePhPr and PMe_2Ph can protrude through the faujasite fragment without any increase in the energy (figures 2a and 2b). On the other hand, $PMePh_2$ is only able to enter the first 12 Å supercage through the 7.5 Å window at the cost of a considerable increase in energy due to the repulsive van-der-Waals interactions which forces the guest molecule into a strained, unfavourable conformation (figure 2c). After an intermediate decrease in energy on the way of the $PMePh_2$ molecule through the first supercage, the energy curve rises again and bends into a plateau. This plateau indicates that the guest molecule is stuck in front of the 7.5 Å aperture to the second supercage. It is pulled forward – and deformed, therewith – but at a point the minimization leads always to the former position and conformation. This behaviour can also be observed in the case of the PPh_3 molecule which does not even enter the first supercage of the faujasite fragment (figure 2d).

3.2. Ship-in-a-bottle approach: FTIR

In order to check these computational results IR experiments were performed in which intrazeolite $[Rh(CO)_2(\mu\text{-}Cl)]_2$ was treated with the phosphine ligands methyldiphenylphosphine ($PMePh_2$), dimethylphenylphosphine (PMe_2Ph), and trimethylphosphine (PMe_3). This complex was chosen because its solution chemistry is well known and it reacts eventually in solution even with an excess of ligand to the carbonyl-containing monomer $[Rh(CO)L_2Cl]$ (table 1) [21,22].

The spectrum of $[Rh(CO)_2(\mu\text{-}Cl)]_2$ sublimated into zeolite DDAY (figure 3a) shows vibration frequencies at 2109, 2093, 2040 and 2006 cm^{-1}. This corresponds very well with a KBr wafer spectrum of this complex. As the preparation method used is similar to the one published by Meyer et al. [23] for intrazeolite $[Rh(CO)_2(\mu\text{-}Cl)]_2$ here the complex should be inside the microporous framework, too. The addition of $PMePh_2$ to this intrazeolite $[Rh(CO)_2(\mu\text{-}Cl)]_2$ leads to the formation of a mixture of substituted rhodium complexes as is indicated by the new IR bands at 2073, 2022, 2000 and 1955 cm^{-1}. This change in the IR spectrum can only be caused by a chemical reaction.

The addition of $PPhMe_2$ to intrazeolite $[Rh(CO)_2\text{-}(\mu\text{-}Cl)]_2$ causes new IR bands at 2020, 1982, 1968, 1956 and 1906 cm^{-1}, whereas the reaction with PMe_3 gives rise to vibration frequencies at 2073, 2022, 1995, 1981 and 1965 cm^{-1}. According to literature data [21,22], the vibration bands below 1990 cm^{-1} can be assigned to dimeric $[Rh_2(CO)_2L_2(\mu\text{-}Cl)_2]$ and monomeric

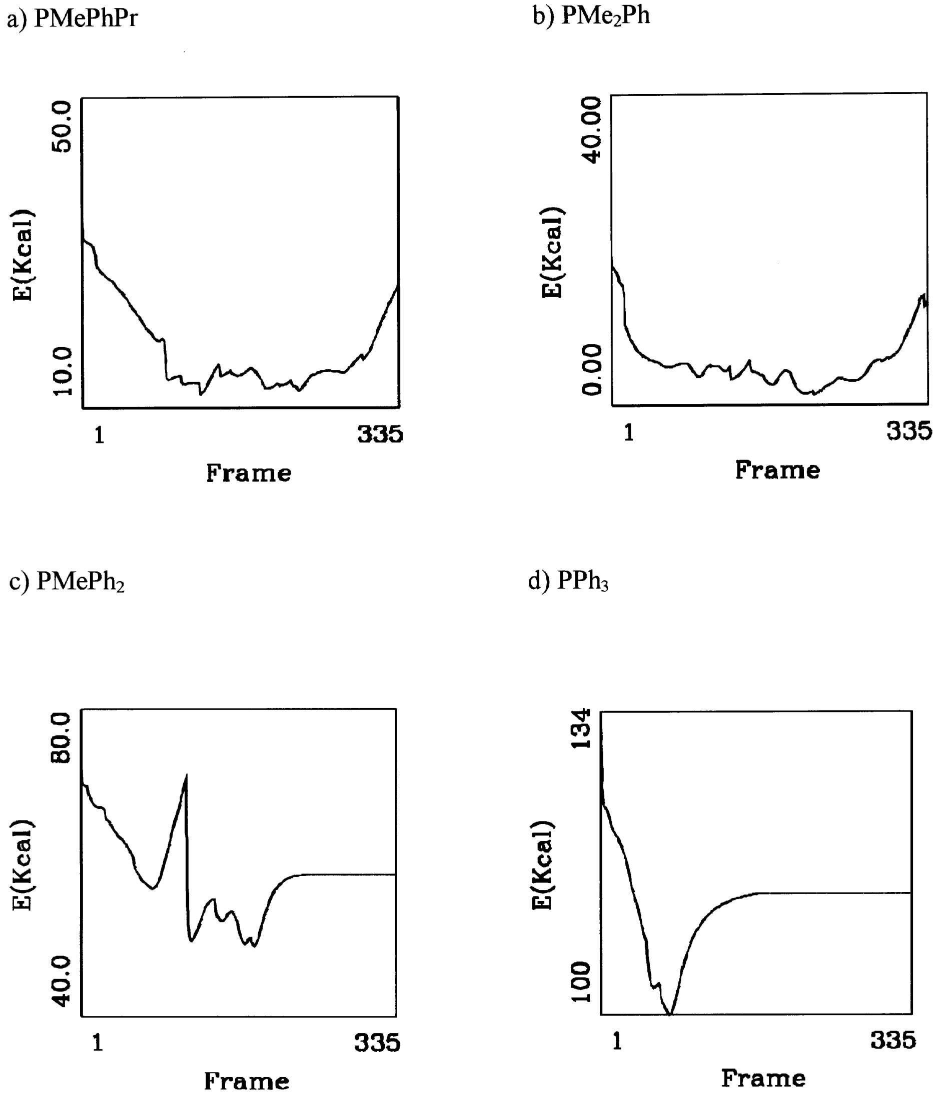

Figure 2. Calculated energy-versus-framework diagrammes of the forced diffusion paths of various phosphines through an all-silica faujasite fragment.

$[Rh(CO)L_2Cl]$. The bands above 1990 cm^{-1} represent dimeric $[Rh_2(CO)_3L(\mu\text{-}Cl)_2]$, monomeric $[Rh(CO)_2LCl]$, and the educt complex.

Independent of an exact assignment, it is clear that in no case a complete reaction of the phosphine ligands with the entrapped $[Rh(CO)_2(\mu\text{-}Cl)]_2$ occurs as this would lead to a single vibration frequency at about 1960 cm^{-1} [21,22]. A comparison of the band intensities indicates the relative ease of the reaction depending on the phosphine used: $PMe_3 < PMe_2Ph < PMePh_2$. In contrast to the computational results in the case of $PMePh_2$ some reaction takes place. This could be due to complex located on the outer surface of the zeolite wafer. A second explanation could be the neglect of framework flexibility in the modeling studies. Surprisingly, even the small PMe_3 ligand does not result in a complete reaction

Table 1
Vibration frequencies of different rhodium complexes resulting from a substitution reaction of $[Rh(CO)_2(\mu\text{-}Cl)]_2$ plus PMe_2Ph [21,22]

Complex	ν_{CO} (cm^{-1})					
$[Rh_2(CO)_2(\mu\text{-}Cl)_2]$	2105(m),	2089(s),	2033(s)			
$[Rh_2(CO)_3L(\mu\text{-}Cl)_2]$		2089(s),	2022(s),		2000(s)	
$[Rh_2(CO)_2L_2(\mu\text{-}Cl)_2]$						1985(s)
$[Rh(CO)_2LCl]$		2094(vs),		2009(s),	2003(vs)	
$[Rh(CO)L_2Cl]$						1964(s)

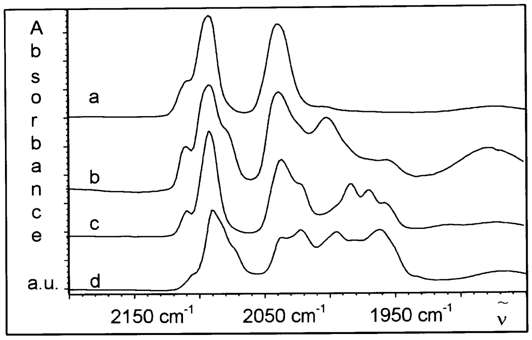

Figure 3. IR spectra of the reaction of $[Rh(CO)_2(\mu\text{-}Cl)]_2$ with various phosphines in DDAY at room temperature: (a) intrazeolite $[Rh(CO)_2(\mu\text{-}Cl)]_2$, (b) $PMePh_2$, (c) PMe_2Ph, (d) PMe_3.

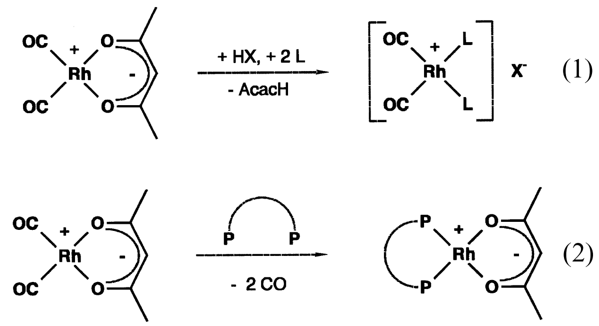

Scheme 1. Homogeneous reactions of $[Rh(acac)(CO)_2]$.

although it is added in large excess. This could be caused by sterical hindrance of the transition state of the substitution reaction in the zeolite micropore system. In a non-microporous environment the reaction would be complete. An increase of the temperature up to 343 K does not change the results above.

3.3. Surface-bonded rhodium complexes: FTIR

As a microporous environment is too narrow to allow the preparation of rhodium phosphine complexes, mesoporous materials in combination with acetylacetonatodicarbonylrhodium(I) were used in an attempt to synthesize surface-bonded rhodium phosphine species. $[Rh(acac)(CO)_2]$ was chosen as rhodium component because of its reactivity: the acetylacetonato ligand can be cleaved off by Brønsted-acids (eq. (1) in scheme 1) [24] and the carbonyl ligands are easily subsituted by phosphines (eq. (2) in scheme 1) [25,26]. An extension of this homogeneous reactivity into the heterogeneous case should be possible.

The vibration bands caused by the carbonyl ligands and by the acetylacetonato ligand of $[Rh(acac)(CO)_2]$ in/on different media are listed in table 2. The solution spectra of $[Rh(acac)(CO)_2]$ show two bands at 2083 and 2015 cm^{-1} in *n*-hexane and 2081 and 2010 cm^{-1} in THF. The more polar solvent causes a slight shift to lower wavenumbers. This solvent effect is pronounced in the case of the vibration frequencies belonging to the acetylacetonato ligand: the higher-frequency band at 1582 cm^{-1} in *n*-hexane shifts to 1574–1567 cm^{-1} in THF. In combination with the different carrier materials the IR bands of the complex shift and new ones appear.

In the case of H(30)USY zeolite the band pair at 2114 and 2048 cm^{-1} can be assigned to the literature-known hydrated zeolite-bound species $[(O_z)(H_2O)Rh(CO)_2]$ [27,28]. Acetylacetonatodicarbonylrhodium reacts under loss of the acetylacetonato ligand with Brønsted-acidic centers of the H(30)USY zeolite. The peaks at 2086 and 2013 cm^{-1} are due to the presence of unreacted $[Rh(acac)(CO)_2]$. The shoulder at 2076 cm^{-1} can be explained by the interaction between carbonyl oxygens and Lewis-acidic centers. The presence of rhodium clusters can be ruled out since there are no bands at 1834 or 1765 cm^{-1} [29].

In the acetylacetonato area signals at 1582, 1571, 1536 and 1526 cm^{-1} are found. The first and the last signal belong to unreacted $[Rh(acac)(CO)_2]$. The band at 1571 cm^{-1} can be explained either by some polar interaction of unreacted $[Rh(acac)(CO)_2]$ with the H(30)USY zeolite or by the presence of acetylacetone. The second proposal is sustained by the vibration frequencies of acetylacetone in H(30)USY: 1589, 1575, 1538 cm^{-1}. So the signals at 1571 and 1536 cm^{-1} are explained by the presence of adsorbed molecular acetylacetone. This means that a part of the rhodium complex has reacted with Brønsted-acidic centers of the zeolite under the formation of acetylacetone.

In case of the carriers Si-MCM-41, Na-MCM-41, NaY and DDAY, which are non- or only very slightly

Table 2

Vibration frequencies of $[Rh(acac)(CO)_2]$ in/on different media. Non-solution spectra were taken after 5 min of vacuum at room temperature

Medium	ν_{CO} (cm^{-1})	ν_{acac} (cm^{-1})
n-hexane	2083(s), 2015(s)	1582(m), 1526(m)
THF	2081(s), 2010(s)	1574–1568(m, br), 1527(m)
Al-MCM-41	2107(sh), 2092(s), 2029(s)	1568(m), 1533(m)
Na-MCM-41	2093(s), 2026(s)	1583(sh), 1568(sh), 1528(m)
Si-MCM-41	2095(s), 2030(s)	1583(sh), 1568(m), 1531(m)
H(30)USY	2114(m), 2086(s), 2078(sh), 2048(m), 2013(s)	1582(m), 1571(w), 1536(sh), 1526(m)
NaY	2098(s), 2078(m), 2032(s), 2000(m)	1561(m), 1525(m)
DDAY	2090(s), 2022(s)	1585(m), 1569(m), 1526(m)

Table 3
Vibration frequencies of acetylacetone in/on different media. Non-solution spectra were taken after 5 min vacuum at 423 K

Medium	ν_{acacH} (cm^{-1})			
film	1729(m), 1710(m), 1622(s, br)			
Al-MCM-41	1726(w),	1591(sh),	1575(m),	1537(ms)
Na-MCM-41	1725(vvw), 1685(vvw),			1541(vvw)
Si-MCM-41		1599(vw),	1574(sh),	1538(w)
H(30)USY		1607(sh), 1589(m),	1575(sh),	1538(ms)
NaY	1731(s), 1696(s),	1594(w),		1539(w)

acidic as could be shown with pyridine adsorption, the carbonyl bands and the acetylacetonate bands in table 2 reveal the presence of unreacted [Rh(acac)$(CO)_2$]. The observed shift of the carbonyl vibration frequencies to higher as well as to lower wavenumbers is not caused by cleavage of the acetylacetonato ligand. The rhodium acetylacetonato bond is intact as is proven by the bands at about 1580 and 1527 cm^{-1}. There are in no case signals at 1574 and 1539 cm^{-1} which can be observed when molecular acetylacetone is adsorbed in/on these carriers. As there are no acidic sites there is no reaction of [Rh(acac)$(CO)_2$] with the surface.

Further support for the above assignment of the carbonyl bands of [Rh(acac)$(CO)_2$] in H(30)USY zeolite is found by extracting this material with methylenechloride. Figure 4 shows the resulting IR spectra. The first spectrum (a) belongs to [Rh(acac)$(CO)_2$] in H(30)USY after 5 min of vacuum at room temperature. The following two spectra were recorded after one (b) and after three (c) extractions with methylenechloride, respectively. The band pair at 2117 and 2052 cm^{-1} assigned to zeolite-bound [$(O_z)(H_2O)Rh(CO)_2$] [27,28] is not influenced, whereas the other signals disappear immediately upon the first extraction. The same is true for the corresponding acetylacetonato bands, i.e. the merely physically adsorbed unreacted complex can be washed out without any problem.

Similar results can be observed with the Al-MCM-41 carrier as the spectra in figure 5 demonstrate. The rather broad carbonyl bands narrow upon extraction with methylenechloride and the maxima change from 2093 and 2029 cm^{-1} in spectrum (a) to 2108 and 2038 cm^{-1} in spectrum (b). The corresponding acetylacetonato band shifts from 1532 to 1538 cm^{-1}. However, in contrast to the H(30)USY sample which is free of unreacted [Rh(acac)$(CO)_2$] after three extractions, here the complex is not completely removed as is proven by the shoulder at 2095 cm^{-1}.

In order to synthesize surface-bonded phosphine complexes the surface-bonded rhodium carbonyl species in Al-MCM-41 were reacted with dimethylphenylphosphine. After the substitution four rather weak peaks at 2093, 2027, 1969 and 1930 cm^{-1} are observed. The first two signals belong to an unidentified strongly adsorbed dicarbonyl complex. The bands below 2000 cm^{-1} can be assigned to mono-substituted species [24,25]. This means that the reaction does not proceed completely which is probably due to sterical constraints at the carrier surface (narrow defects, hindered transition states). Attempts to carry out the same reaction in the micropore system of a faujasite type zeolite led to considerably less conversion. Temperature increase up to 343 K gave the same results.

3.4. Surface-bonded rhodium complexes: ^{31}P MAS NMR

In a second approach in order to obtain surface-bonded phosphine complexes, the rhodium phosphine bond is prepared in solution before heterogenization. Therefore, a calculated amount of [Rh(acac)(chira-

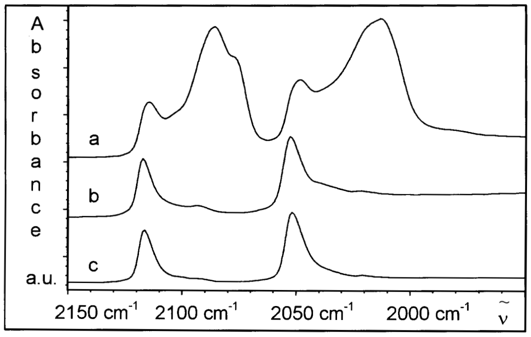

Figure 4. IR spectra of [Rh(acac)$(CO)_2$] in H(30)USY: (a) 5 min vacuum at room temperature, (b) 1 extraction with CH_2Cl_2, (c) 3 extractions with CH_2Cl_2.

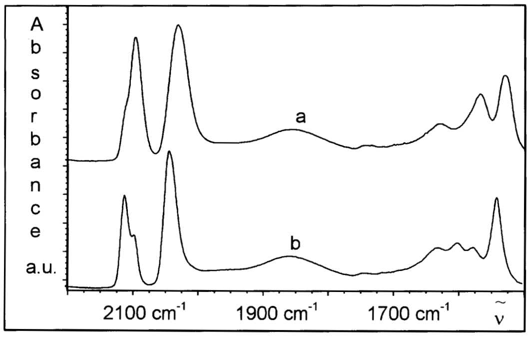

Figure 5. IR spectra of [Rh(acac)$(CO)_2$] in Al-MCM-41: (a) after 5 min vacuum at room temperature, (b) 3× washed with CH_2Cl_2.

phos)] corresponding to the number of acid sites of a given Al-MCM-41 (0.062 mmol/g according to NH_3-desorption) was reacted with the carrier in methylenechloride. The solution is completely de-coloured after 30 min. After three extractions with methylenechloride, IR and ^{31}P MAS NMR spectra of the material were recorded. The NMR spectrum is presented in figure 6.

The chemical shift of the free chiraphos ligand in solution is $\delta = -9.1$ ppm (s). Upon complexation in [Rh(acac)(chiraphos)] it becomes 60.78 ppm (d, $^1J_{\mathrm{Rh-P}} = 131.9$ Hz). The MAS NMR spectrum of the rhodium chiraphos species in Al-MCM-41 shows a broad signal at 59.5 ppm (s) with spinning side bands. This is very similar to the chemical shift in the educt complex. Since the rhodium phosphorus coupling is too small to be seen under these conditions, the NMR spectrum confirms that the rhodium phosphine bond is not affected during the surface reaction. No NMR detectable free ligand is present. The IR spectrum of the same material answers the question, whether this rhodium chiraphos species is present as an acetylacetonato complex or as a surface-bonded complex. The absence of vibrations at 1580 and 1526 cm^{-1} in the IR spectrum proves that there is no rhodium acetylacetonato bond. This leads to the conclusion that the rhodium chiraphos species must be bonded directly to surface oxygens of the support. In correspondence to the surface-bonded carbonyl complex, we assume it is a $[(O_s)_x$–Rh(chiraphos)] species.

4. Conclusions

The micropore system of dealuminated faujasite type zeolite DAY is too small according to computer modeling and IR studies to allow a controlled reaction of entrapped $[Rh(\mu\text{-}Cl)(CO)_2]_2$ with various methylphenylphosphines $PMe_{3-x}Ph_x$ to a uniform product. The synthesis of surface-bonded rhodium phosphine complexes in mesoporous aluminium-containing and therefore acidic MCM-41 material is possible. In neutral all-silica MCM-41 no surface reaction takes place. The procedure in which the phosphine complex synthesis in solution precedes the immobilization reaction in Al-MCM-41 is preferred to the opposite order, as the latter route gives merely an incomplete conversion. The surface-bonded rhodium chiraphos species in Al-MCM-41 have been prepared and identified as $[(O_s)_x$–Rh(chiraphos)] by IR and ^{31}P MAS NMR spectroscopy.

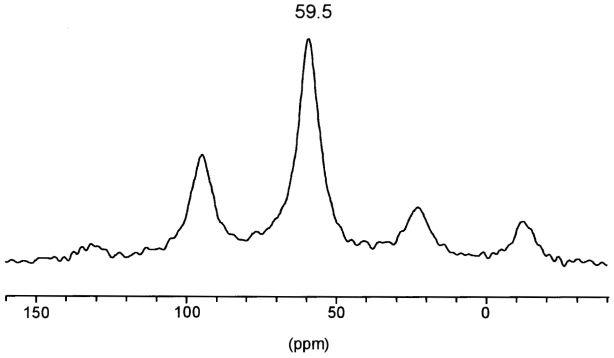

Figure 6. ^{31}P MAS NMR spectrum of rhodium chiraphos species in Al-MCM-41.

Acknowledgement

The authors wish to thank the Deutsche Forschungsgemeinschaft for financial support in the course of the SFB 380. Furthermore we are grateful to Dr. Zibrowius for performing the MAS NMR measurements.

References

[1] D.C. Bailey and S.H. Langer, Chem. Rev. 81 (1981) 109.
[2] S.L. Scott and J.M. Basset, J. Mol. Catal. 86 (1994) 5.
[3] Y.I. Yermakov, J. Mol. Catal. 21 (1983) 35.
[4] A. Zecchina and C.O. Arean, Catal. Rev. Sci. Eng. 35 (1993) 261.
[5] T.N. Huang and J. Schwartz, J. Am. Chem. Soc. 104 (1982) 5244.
[6] Th. Maschmeyer, F. Rey, G. Sanker and J.M. Thomas, Nature 378 (1995) 159.
[7] R. Parton, D. de Vos and P.A. Jacobs, in: *Zeolite Microporous Solids: Synthesis, Structure, and Reactivity*, eds. E.G. Derouane et al. (Kluwer Academic, Dordrecht, 1992) p. 555.
[8] N. Herron, G.D. Stucky and C.A. Tolman, Inorg. Chim. Acta 100 (1985) 135.
[9] B.V. Romanovsky and V.Y. Zakharov, Khim. 18 (1977) 142.
[10] N. Herron, Inorg. Chem. 25 (1986) 4741.
[11] D.J. Chatterjee, H.C. Bajaj, A. Das and K. Bhatt, J. Mol. Catal. 92 (1994) L235.
[12] D.C. Tomczak, V.L. Zholobenko, H. Treviño, G.D. Lei and W.M.H. Sachtler, in: *Zeolites and Related Microporous Materials: State of the Art 1994*, eds. J. Weitkamp, H.G. Karge, H. Pfeiffer and W.F. Hölderich, Stud. Surf. Sci. Catal. 84 (1994) 893.
[13] G. Bergeret, P. Gallezot, P. Gelin, Y. Ben Taarit, F. Lefebre, C. Naccache and R.D. Shannon, J. Catal. 104 (1987) 279.
[14] Th. Bein, S.J. McLain, D.R. Corbin, R.D. Farlee, K. Moller, G.D. Stucky, G. Woolery and D. Sayers, J. Am. Chem. Soc. 110 (1988) 1801.
[15] G.A. Ozin, D.M. Haddleton and C.J. Gil, J. Phys. Chem. 93 (1989) 6710.
[16] G.A. Ozin and C. Gil, Chem. Rev. 89 (1989) 1749.
[17] J. Beck, J. Vartuli, W. Roth, M. Leonowicz, C. Kresge, K. Schmitt, C. Chu, D. Olson, E. Sheppard and S. McCullen, J. Am. Chem. Soc. 114 (1982) 834.
[18] S.J. Beck, D.C. Calabro, S. McCullen, B.P. Pelrine, K.D. Schmitt and J.C. Vartuli, US patent 5,145,816 (1992).
[19] Z. Luan, C.-F. Cheng, W. Zhou and J. Klinowski, J. Phys. Chem. 99 (1995) 1018.
[20] A. Janssen, PhD thesis, RWTH Aachen, Germany (1996).
[21] J. Gallay et al., J. Organomet. Chem. 38 (1972) 179.
[22] A.J. Deeming and P.J. Sharratt, J. Organomet. Chem. 99 (1975) 447.

[23] W. Meyer, G. Vorbeck, L.J.M. van de Ven, J.W. de Haan, R.A. van Santen and W. Keim, in: *Book of Abstracts of the 7th German Zeolite Conf.*, 7. Deutsche Zeolithtagung, Konstanz 1995, Po45.

[24] D. Sinou and H.B. Kagan, J. Organomet. Chem. 114 (1976) 325.

[25] A.M. Trzeciak and J.J. Ziolkowski, Inorg. Chim. Acta Lett. 64 (1982) L267.

[26] G.J.H. Buisman, E.J. Vos, P.C.J. Kamer and P.W.N.M. van Leeuwen, J. Chem. Soc. Dalton Trans. (1995) 409.

[27] F. Lefebre and Y. Ben Taarit, Nouv. J. Chem. 8 (1984) 387.

[28] K.J. Balkus and K. Nowinska, Microporous Materials 3 (1995) 665.

[29] E.J. Rode, M.E. Davis and B.E. Hanson, J. Catal. 96 (1985) 574.